NUMERICAL INVESTIGATION OF A MECHANICAL DEVICE SUBJECTED TO A DEFLAGRATION-TO-DETONATION TRANSITION

Beccantini A.[1,*], Galon P.[2], Faucher[2]
[1] CEA, DEN, DM2S/SFME, F-91191 Gif-sur-Yvette Cedex, France
[2] CEA, DEN, DM2S/SEMT, F-91191 Gif-sur-Yvette Cedex, France
[*] Corresponding author: alberto.beccantini@cea.fr

ABSTRACT

In this work we evaluate the consequences of the combustion of a stoichiometric mixture of hydrogen-air on a mechanical device which can be considered as a long tube. In order to choose the most dangerous combustion regime for the mechanical device, we devote a particular attention to the investigation of the 1D deflagration-to-detonation transition. Then, once established the most dangerous combustion regime, we compute the reacting flow and the stress and strain in the mechanical device. Analyses are performed using both semi-analytical solutions and Europlexus, a computer program for the simulation of fluid-structure systems under transient dynamic loading.

1 Introduction

The purpose of this work is to evaluate the consequences of the combustion of a stoichiometric mixture of hydrogen-air on a mechanical device. This mechanical device can be considered as a long tube filled with an irregular set of obstacles with a negligible block ratio. Amongst the most dangerous combustion regimes, we have to consider the one in which a deflagration is initiated in one extremity of the tube and there is a detonation transition due to the presence of obstacles (or to the tube roughness); another dangerous regime is the detonation initiation due to the shock reflection at the other extremity. The distance between the point of initiation of the deflagration and the point at which the transition occurs is called run-up distance; its value depends on the nature of the mixture and the geometry [1]. Since the run-up distance in our device is not known, we do not perform any hypothesis concerning the combustion regime; instead, using a simplified mechanical device, we find the most critical combustion regime and then we verify if the tube integrity is guaranteed in this combustion regime.
The report is divided as follows. In Section 2 we describe the problem we deal with as well the way of modelling the problem. In Section 3 we deeply discuss the deflagration-to-detonation transition in a close 1D geometry. Finally, in Section 4 we briefly present the result for most critical combustion regime acting on the mechanical device. Conclusion follows.

2 Problem

We consider a 7 m tube with a 0.245 m inner radius. The left extremity is open and connected to a large containment; the right extremity is closed and present an ellipsoidal shape . The thickness of the tube is constant and equal to 8.17 mm. As already mentioned, the tube is filled with a stoichiometric mixture of hydrogen and air with $P = 1.2$ bar, $T = 290$ K. We want to investigate the effects of the hydrogen-air combustion in this tube.

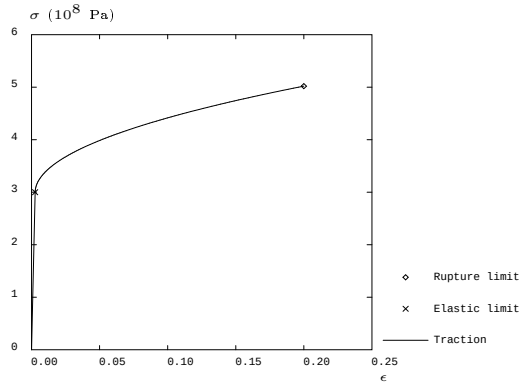

Figure 1: Isotropic von Mises material. Stress-strain law.

2.1 Choice of the initiation point

If the extremities were both closed, the most dangerous initiation point would be at one of the extremities. Since one extremity (the left one) is open, the initiation of the combustion in this point is not so important. Indeed, the flame is not accelerated and the burnt gas is pushed outside from the tube. If the combustion is initiated between the left and the right extremity, we have two flames propagating toward the two extremities, preceded by their precursor shock. Once the left travelling precursor shock reaches the left open extremity, a rarefaction wave enters the domain and, if it reaches the right travelling flame, it weakens the flame and then its precursor shock. A more realistic choice of the initiation point is then function of the flame speed and the way in which the combustion occurs. For this reason, conscious of the fact that the pressure load thus determined will be more dangerous for the structure than the real one, we choose as initiation point the left extremity of the tube and we suppose that this extremity is closed.

2.2 Material properties

Concerning the tube, the material properties (in the order density, Poisson coefficient ν, Young modulus E, the elastic limit (elastic limit stress $\sigma = (R^t_{\mathrm{p0,2}})_{\min}$ and elastic limit strain $\epsilon = (R^t_{\mathrm{p0,2}})_{\min}/E$) and the rupture limit (rupture limit stress $\sigma = (R_{\mathrm{m}})_{\min}$ and rupture limit strain $\epsilon = (A_{\mathrm{t}})_{\min}$)) are given in the following table (for the meaning of these notations, one can see [2]).

ρ	ν	E	$(R^t_{\mathrm{p0,2}})_{\min}$	$(R^t_{\mathrm{p0,2}})_{\min}/E$	$(R_{\mathrm{m}})_{\min}$	$(A_{\mathrm{t}})_{\min}$
7850. kg/m^3	0.33	113.2E9 Pa	300E6 Pa	0.27%	502E6 Pa	20%

The material obeys to the isotropic von Mises material law of Figure 1.

As far as the gas is concerned, we perform the same hypotheses as in [3]: all the gases involved can be considered thermally perfect; the chemical reaction governing the combustion is a global chemical reaction and is supposed to be irreversible; we can neglect viscous effects, thermal and species diffusion (the flame is considered an infinitely thin surface (infinitely fast reaction) with a given fundamental speed).

2.3 Choice of the initial condition and modelling

As already mentioned, we do not know the regime at which the combustion occurs; for this reason, we must take into account all the possible combustion regimes. In order to avoid to perform a large number of multidimensional computations (computations which are

excessively time consuming if we want to provide mesh independent results), we proceed as follows.

1. We consider different combustion regimes (investigated in Section 3). As shown in the figure below, in each case a 1D combustion is initiated in the left side of the domain and we compute the pressure as function of time on the right side of the domain (where the strongest reflection occurs). At this stage, we do not take into account the tube deformation.

2. Then, as shown in figure below, we apply this pressure as function of time to an infinite cylinder in axisymmetric deformation with the same radius and the same material properties as the tube (i.e. we apply to the infinite cylinder a time-dependent uniform load).

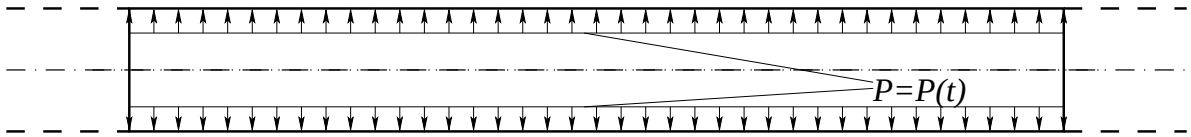

   In this way, we can have an idea of which kind of combustion regime is more dangerous for the device. Moreover, we provide stresses and strains which we expect to be larger than the ones obtained in the mechanical device, if we exclude the regions in which we can have strain concentrations or in which bending is important.

3. Finally, once determined the most critical combustion regime for the infinite cylinder, we compute the flow inside the mechanical device and the stress and strain due to such flow. Note that at this stage we take into account the effects of the deformation of the tube on the flow (although in this particular case it is not sensibly important). We also emphasize that, at this stage, bending is taken into account.

In the following, the combustion regime analysis is performed using both semi-analytical solutions (obtained as in Section 6.1 of [3]) and numerical computations; the numerical computations are performed using the Reactive Discrete Equation method, developed in [7] to investigate the propagation of evaporation fronts and adapted in [3] to investigate the flame front propagation. Second order in space and time is achieved using a predictor-corrector technique presented in [8]. The Reactive Discrete Equation method is implemented, in an Arbitrary Lagrangian Eulerian approach, in the Europlexus code [9], a computer program for the simulation of fluid-structure systems under transient dynamic loading. The "solid" tube is investigated using the Finite Element method, in which the pressure load is given by the gas flow computation; on the other hand, the inner part of the tube, which represents the border for the domain occupied by the gas mixture, moves because of the action of the pressure. We emphasize that the computations are realized using differently refined meshes (with a Courant number equal to 0.75), in order to verify the mesh independence of the provided numerical results.

3 1D deflagration-to-detonation transition

All the analyses presented in this section are based on the model of a 1D constant speed flame acting as a porous piston (see [1], Paragraph 1.2). This model (called "steady flame" in [10], or "unsteady double discontinuity" in Paragraph 1.2.2 of [1]) is described Section 3.1.

By varying the flame velocity, it is possible to explore all the combustion regimes, from the slow deflagration to the detonation (see also Figure 6 in [1]). This velocity is not the laminar burning velocity, but an effective velocity, which takes into account that the flow can be turbulent and the flame surface is not plane. We proceed in this way because a direct modelling of the flow in the real geometry is impossible, so we have to explore all the combustion regimes. At the same manner, since we do not know where and how the deflagration-to-detonation occurs, in Section 3.2 we consider the case in which the detonation occurs instantaneously at the flame; in Section 3.3 we consider the case in which the detonation is initiated by the reflection of the precursor shock. As we will see, in the last case we generate an overdriven detonation (even if the wall is fixed).

3.1 Steady deflagration

We consider a constant (fundamental) speed deflagration wave moving in a 1D tube. The solution is function of

$$\mathbf{U} = \mathbf{U}(x, t; L, K_0, P_0, T_0, R_u, R_b, c_{v,u}(T), c_{v,b}(T), h_u^0 - h_b^0) \tag{1}$$

where $\mathbf{U}$ is the vector of the conservative variables (densities of the single components, total momentum, total energy), x is the abscissa (distance from the left extremity of the tube), t is the time last from the deflagration initiation, K_0 is the fundamental speed, L is the total length of the tube, P_0 and T_0 are the unperturbed conditions for the unburnt mixture, R_u , R_b, $c_{v,u}$, $c_{v,b}$ are respectively the gas constant and the constant volume specific heats capacities for the unburnt and burnt mixture[1], $(h_u^0 - h_b^0)$ the difference between the formation enthalpies (evaluated at 0 K) for the unburnt and burnt mixture. Using the dimensionally-independent reference quantities P_0, T_0, L and R_u we obtain that the non-dimensional conservative variables can be written as function of

$$\begin{aligned} \tilde{\mathbf{U}} &= \tilde{\mathbf{U}}\left(\frac{x}{L}, \frac{t\sqrt{R_u T_0}}{L}; 1, \frac{K_0}{\sqrt{R_u T_0}}, 1, 1, 1, \frac{R_b}{R_u}, \frac{c_{v,u}\left(\frac{T}{T_0}\right)}{R_u}, \frac{c_{v,b}\left(\frac{T}{T_0}\right)}{R_u}, \frac{q}{R_u T_0}\right) \\ &= \tilde{\mathbf{U}}\left(\tilde{x}, \tilde{t}; \tilde{K_0}, \frac{R_b}{R_u}, \frac{c_{v,u}\left(\frac{T}{T_0}\right)}{R_u}, \frac{c_{v,b}\left(\frac{T}{T_0}\right)}{R_u}, \frac{q}{R_u T_0}\right) \end{aligned} \tag{2}$$

with $q = h_u^0 - h_b^0$ being the chemical energy released per unit mass. Then the non-dimensional solution depends on the non-dimensional variables $\tilde{x}$ and $\tilde{t}$ and on 5 non-dimensional parameters. Since the gas mixture and the initial conditions are given, we have to investigate the solution with respect to one parameter only, the ratio between the fundamental flame speed and the reference speed.

Before the interaction of the precursor shock with the right wall, the solution is self similar. In Figures 2 we present different cases: a weak deflagration wave (WDF, with $\tilde{K_0}$ equal to 0.5), some Chapman-Jouguet deflagrations (CJDF, with $\tilde{K_0}$ equal to 0.6, 0.7, 0.85 and 1.1) and a Chapman-Jouguet detonation (CJDT, non sensibly different from the CJDF with $\tilde{K_0}$ equal to 1.1). See Section 6.1 of [3] for details.

We emphasize that, in the case $\tilde{K_0} = 0.6$ the temperature behind the precursor shock is about 880 K; in the case $\tilde{K_0} = 0.7$ the temperature behind the precursor shock is about 1000 K; in the case $\tilde{K_0} = 0.85$ the temperature behind the precursor shock is 1260 K[2]. It could be pointed out that a mixture of hydrogen-air spontaneously burns for temperatures larger than 1000 K. In the case $\tilde{K_0} = 0.85$, at the state behind the precursor shock the delay

[1] Strictly speaking, the specific heats are not parameters but function of T. Often, these functions are approximated using temperature polynomials. Then, if we use 4-th order temperature polynomials, each c_v involves 5 parameters.

[2] As already mentioned, the reference value of the temperature is 290 K.

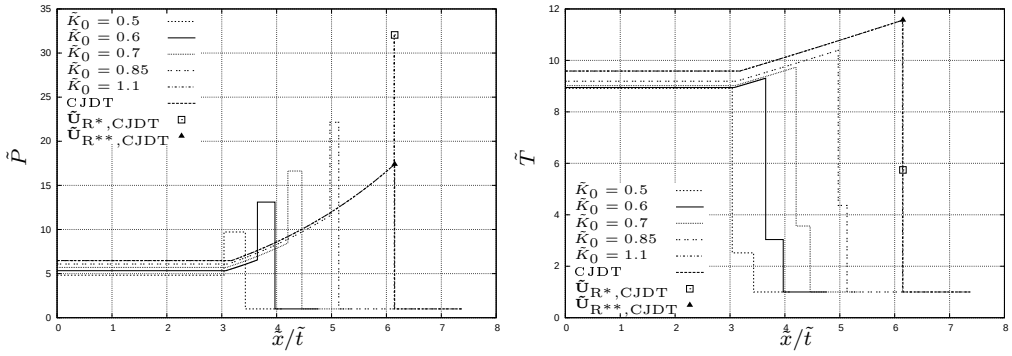

Figure 2: 1D plane-symmetric steady flame (flow before the interaction of the precursor shock with right wall). $\tilde{P}$ and $\tilde{T}$ versus $\tilde{x}/\tilde{t}$ for different values of $\tilde{K}_0$. (Non-dimensional values).

time of burning (τ_d) is of the order of $1 - 10$ μs [4, 5]. It follows that, when a fluid element keeps between the precursor shock and the flame for a time larger that the induction time, it starts burning. It follows that, if we take $\tau_d = 10$ μs, the maximum distance between the shock and the flame is $K_0\tau_d \approx 2$ mm; once this maximum distance is reached, the flame and the precursor shock keeps coupled and we have a detonation transition at the flame; i.e. the case $\tilde{K}_0 = 0.85$ cannot exist. Nevertheless, for the sake of completeness, we sometimes investigate deflagrations with $\tilde{K}_0 = 0.85$.

3.2 DDT at the flame

The combustion is initiated in the (closed) left extremity of the tube (see Figure 3) and moves forward with a fundamental speed equal to K_0. At $x = L_d$ we have the transition to the detonation regime. According to the dimensional analysis, since the gas mixture and the initial conditions are given, we have to investigate the solution with respect to two parameters only, the non-dimensional fundamental flame speed and the non-dimensional point at which the deflagration-to-detonation transition occurs.

3.2.1 Infinitely slow flame

If $K_0/(\sqrt{R_u T_0}) \approx 0$, the dependence from this non-dimensional parameter can also be neglected. In this case the flame behaves like an infinitely slow permeable and adiabatic piston, which transfers mass from the unburnt region (index u in the following) to the burnt region (index b in the following) and does not exchange any heat by hypothesis (see Figure 4).
We can distinguish between two stages: in the first stage, the flame moves at slow speed until a certain point; at this point, we postulate that the transition to detonation occurs (second stage). As the combustion occurs in the first stage, the pressure in the closed tube increases. Then, the transition to the detonation regime occurs in a pre-compressed gas. That is, the longer the distance at which the transition occurs, the larger the maximum overpressure. Conversely, the longer the distance at which the transition occurs, the lower the characteristic time at which the overpressure acts on the tube walls. Since the damage on a structure depends both on the maximum overpressure and on the positive impulse, we

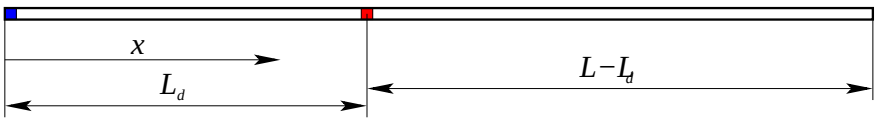

Figure 3: DDT at the flame. The domain. The combustion is initiated in the left extremity (blue point) and the transition to the detonation regime occurs instantaneously at $x = L_d$ (red point).

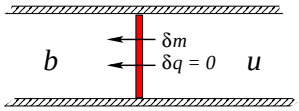

Figure 4: DDT at the flame. Infinitely slow moving flame (in red), two region model. On the left, the burnt region (b). On the right, the unburnt region (u).

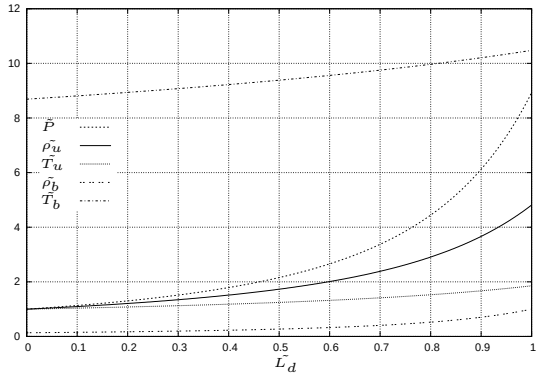

Figure 5: DDT at the flame. Infinitely slow moving flame. Stage 1. Computation of the burnt and unburnt states as function of $\tilde{L_d}$.

expect an extremal value between the value $\tilde{L}_d = 0$ and $\tilde{L}_d = 1$ (in the case $\tilde{L}_d \approx 1$ we have the same consequence as a slow AICC).
Let us now describe the governing equation in first stage. Since the combustion occurs at low speed, the pressure can be considered constant in space [6] (it increases as $\tilde{L}_d$ does). Then the equation of state gives

$$P = \rho_u R_u T_u = \rho_b R_b T_b. \tag{3}$$

The equations of conservation of the total mass and the total energy are

$$L_d\rho_b + (L - L_d)\rho_u = L\rho_0 \tag{4}$$

$$\left(L_d\rho_b \int_0^{T_b} \mathrm{d}\tau \left\{c_{v,b}(\tau)\right\}\right) + \left((L - L_d)\rho_u \int_0^{T_u} \mathrm{d}\tau \left\{c_{v,u}(\tau)\right\}\right) = L\rho_0 \int_0^{T_0} \mathrm{d}\tau \left\{c_{v,u}(\tau)\right\} + L_d\rho_b q. \tag{5}$$

Then, we have to consider that in the unburnt mixture an isentropic compression occurs, i.e.

$$0 = \delta q = c_{v,u}\mathrm{d}T_u - \frac{P}{\rho_u^2}\mathrm{d}\rho_u, \quad \text{i.e.} \quad 0 = \frac{1}{\gamma_u(T_u) - 1}\frac{\mathrm{d}T_u}{T_u} - \frac{\mathrm{d}\rho_u}{\rho_u} \tag{6}$$

To conclude we have to determine P, ρ_u, T_u, ρ_b and T_b (five unknowns) as function of L_d and we have five conditions (equations (3), (4), (5), (6)). In Figure 5 we present the burnt and unburnt states as function of $\tilde{L_d}$. As one can see, as $\tilde{L}_d = 1$, the pressure reach the so called AICC values.
Once computed the first stage, we compute the detonating flow (and the pressure acting on the right wall) numerically.

3.2.2 Fast flame

Before the interaction of the precursor shock with the right wall, the solution is self similar. We consider some of the cases presented in Section 3.1; we do not take into account the

cases in which the temperature behind the precursor shock is higher than 1000 K (i.e. we only consider the cases with $\tilde{K}_0$ equal to 0.5, 0.6, 0.7). Let us consider the case in which the transition occurs such that the precursor shock and the generated detonation reach the wall at the same time. We call $\tilde{L}_{d,\mathrm{foc}}$ this "critical" value for $\tilde{L}_d$ ("foc" stands for focusing). This value depends on $\tilde{K}_0$ and increases with $\tilde{K}_0$. In the case of the WDF with $\tilde{K}_0 = 0.5$, $L_{d,\mathrm{foc}} \approx 0.83$. Let us present the pressure at different times (see Figure 6). As the DDT develops at the flame, the pressure increases and we have a CJDT travelling towards the right wall, which follows the right-travelling precursor shock. At the same time, we have a weak left-travelling shock wave in the burnt gas. At $\tilde{t} \approx 0.020$ we have the interaction of both the precursor shock and the CJDT with the right wall, which creates a (non-dimensional) pressure of about 275 (see also Figure 7, in which we represented the non-dimensional pressure as function of

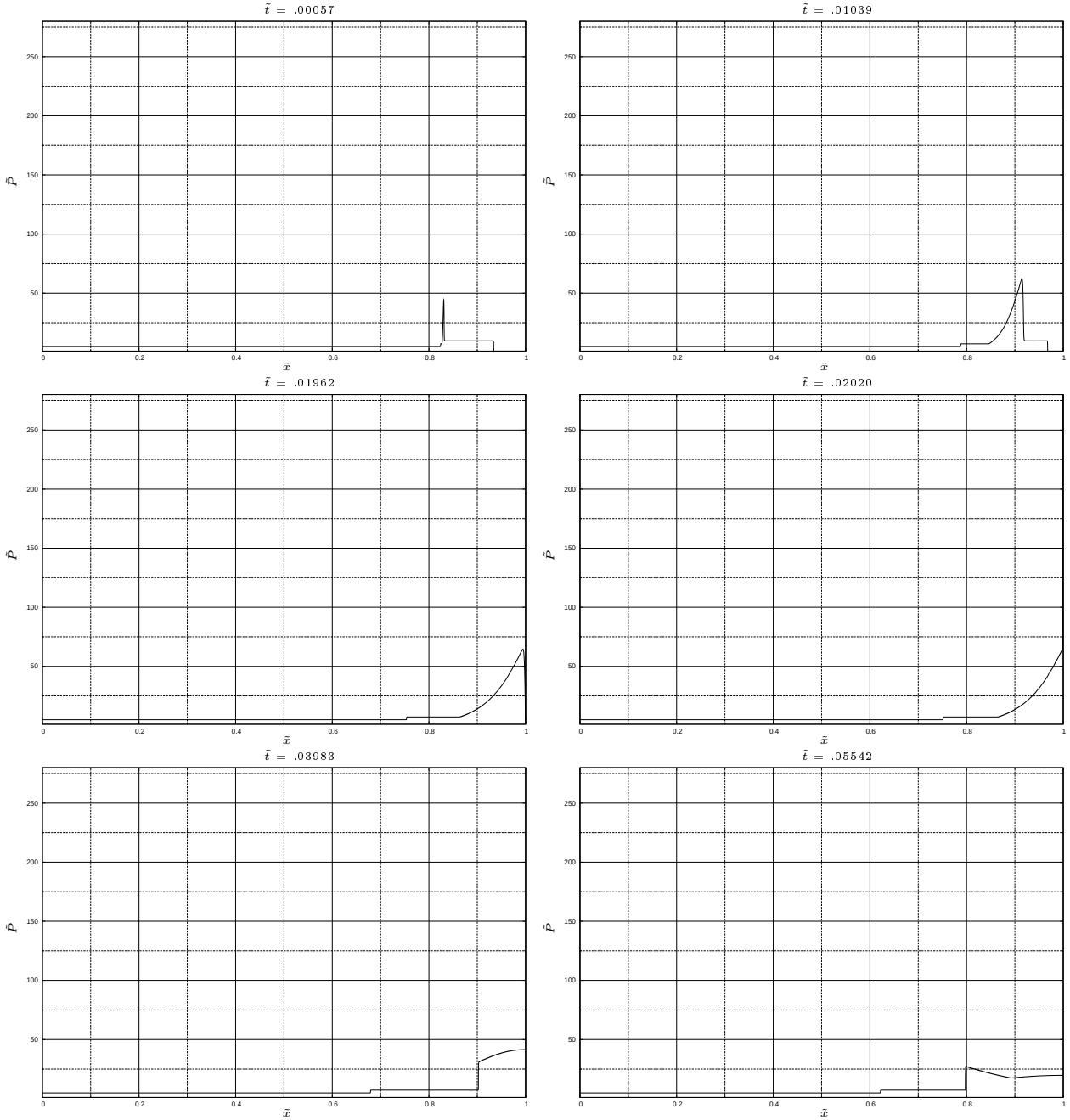

Figure 6: DDT at the flame. $\tilde{K}_0 = 0.5$. $\tilde{L}_d = \tilde{L}_{d,\mathrm{foc}} \approx 0.83$. Pressure $\tilde{P}$ as function of $\tilde{x}$ at different times. The maximum pressure is reached as the precursor shock and the detonation wave are simultaneously reflected by the right wall at $\tilde{t} \approx .02$; its value is about 275. (Non-dimensional values).

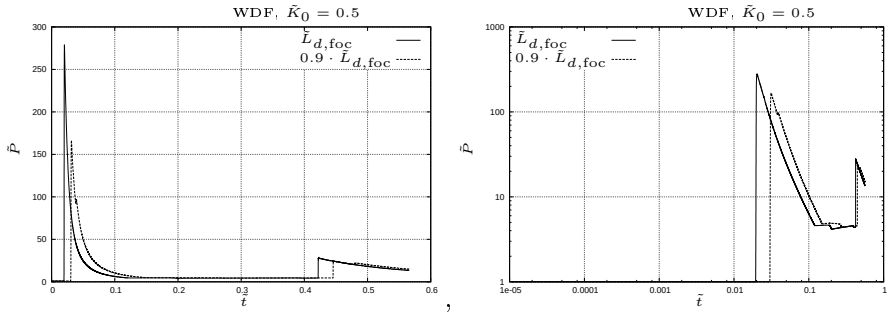

Figure 7: DDT at the flame. Pressure $\tilde{P}$ as function of $\tilde{t}$ on the right extremity. (Non-dimensional values).

the non-dimensional time in the right extremity); then the pressure decreases because of the interaction of the Taylor wave with the wall.
In order to investigate the sensitivity analysis of the solution with respect to $\tilde{L}_d$, we suppose that the the detonation transition occurs at $\tilde{L}_d = 0.9\tilde{L}_{d,\mathrm{foc}}$. In this case, when the detonation reaches the precursor shock and enter in the non-precompressed region, since the the flow behind the Taylor wave is no more sonic in the flame frame, a new rarefaction wave is originated. This new Taylor wave weakens the detonation wave, until it reaches a new CJDT state (the CJDT state in the unperturbed mixture). The overpressure at the right wall results to be lower than in the previous case (see Figure 7). From a qualitative point of view, we have the same behavior in the cases of CJDF with $\tilde{K}_0 = 0.6$ and 0.7. Concerning the pressure as function of the time on the right extremity of the tube, for $\tilde{L}_d = \tilde{L}_{d,\mathrm{foc}}$, if we increase $\tilde{K}_0$ we increase the maximum overpressure but at the same time we decreases the time duration of the first reflection.

3.3 Detonation initiation due to the shock reflection

It is well know that the reflection of the precursor shock can cause the initiation of a detonation wave (see for instance [11]). Here we restrict our attention to the case of a precursor shock generated by a steady flame in a 1D plane geometry (Figure 2). According to the dimensional analysis, since the gas mixture and the initial conditions are given, we have to investigate the solution with respect to one parameter only, i.e. $\tilde{K}_0$, (non-dimensional fundamental flame speed).
We take as initial time ($t = 0$) the instant in which the flame is generated in the left extremity. We can consider three different stages.

1. Before the reflection with the right extremity, the solution consists in a steady flames moving at constant speed.

2. The impact of the precursor shock with the wall occurs at

$$t_{\mathrm{imp}} = \frac{L}{D_{\mathrm{sw}}}$$

D_{sw} being the speed of the precursor shock of a flame moving with visible speed equal to D and fundamental speed equal to K_0. We emphasize that the visible flame speed is lower than the shock speed, namely $D \leq D_{\mathrm{sw}}$; the case $D = D_{\mathrm{sw}}$ corresponds to the case of detonation. According to the hypothesis here considered, the impact of the precursor shock with the wall generates a detonation wave, moving with speed D'_{CJDT} toward the incoming flame. The flame-detonation interaction occurs at $t = t_{\mathrm{imp}} + \Delta t$, with Δt satisfying the following equation

$$(Dt_{\mathrm{imp}}) + (D\Delta t) = L - (D'_{\mathrm{CJDT}}\Delta t), \quad \text{i.e} \quad \Delta\tilde{t} = \frac{1}{\tilde{D}_{\mathrm{sw}}} \frac{\frac{\tilde{D}_{\mathrm{sw}}}{\tilde{D}} - 1}{1 + \frac{\tilde{D}'_{\mathrm{CJDT}}}{\tilde{D}}}$$

As one can see, if the right travelling flame is a detonation wave, it is $\tilde{D} = \tilde{D}_{\text{sw}}$ and stage 2 does not exists ($\Delta\tilde{t} = 0$).

3. The interaction of the right travelling flame with the left travelling detonation wave generates a non reactive flow (everything is already burnt) consisting in left and right travelling shock waves.

The solution of the flow in stages 1 and 2 can be determined semi-analytically (using the same strategy as in Section 6.1 of [3]); then we compute the non reactive flow after the interaction between the right travelling flame and the left travelling detonation.
In general, we can say that the larger the visible flame speed $\tilde{D}$ (or the fundamental speed $\tilde{K}_0$) in the stage 1, the stronger the precursor shock, the stronger the (total) energy density between the flame and the precursor shock, the lower the distance between the flame and the precursor shock. Then, the larger the visible flame speed $\tilde{D}$, the stronger the left travelling detonation wave. Moreover, the larger the fundamental flame speed $\tilde{K}_0$, the lower $\tilde{\Delta}t$. If we look for structure damages, we expect that the worst case is between the two extreme cases $\tilde{K}_0 = 0$ and $\tilde{K}_0 \approx 1.1$. As already mentioned in Section 3.1, some of these cases can be excluded from the fact that the temperature behind the precursor shock cannot be larger than 1000 K, because of the autoignition of the mixture. If $\tilde{K}_0 = 0.7$, the temperature behind the precursor shock is about 1000 K, so that this value could be considered as a physical border for our study. Nevertheless, for the sake of completeness, the case $\tilde{K}_0 = 0.85$ (temperature behind the precursor shock equal to 1200 K) will also be considered.
In Figure 8 we present the solution in different cases before the interaction between the left travelling detonation with the right travelling flame (i.e. at the end of the stage 2). In the

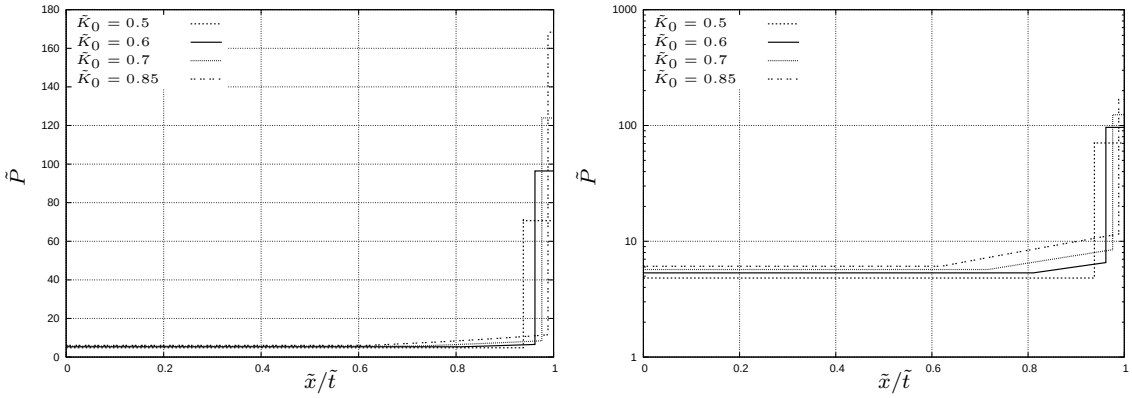

Figure 8: Detonation initiation due to the shock reflection. Solution before the interaction of the left travelling detonation with the right travelling flame. $\tilde{P}$ and $\tilde{T}$ versus $\tilde{x}/\tilde{t}$ for different values of $\tilde{K}_0$. On the bottom, logarithmic scale. (Non-dimensional values).

case of $\tilde{K}_0 = 0.5$, $\tilde{\Delta}t = 0.0169$ and the (non-dimensional) CJDT pressure equal to 70; in the CJDF cases, it is $\tilde{K}_0 = 0.6$, 0.7, 0.85, $\tilde{\Delta}t = 0.0116$, 0.00787, 0.00401 and the (non-dimensional) CJDT pressure equal to 95, 120, 170.
We emphasize that the left travelling detonation wave can be in strong regime (SDT). This is due to the fact that it travels in a unburnt gas which is not at rest but moves towards the right wall. It follows that, in a Galilean frame fixed with the unburnt gas, the right wall moves toward the left, which can generate a overdriven (strong) detonation. In the cases here represented, we have a CJDT detonation in the first case ($\tilde{K}_0 = 0.5$); but even in this case the pressure behind the Taylor wave is 70.7 and the pressure in the CJDT state is 71.2 (i.e. the right extremity velocity in the unburnt gas frame is close to the velocity in the CJDT state). In the other cases the detonation is in the overdriven (strong) regime.
In Figure 9 we present the pressure as function of the time on the right wall (here we take as $t = 0$ the instant in which there is the impact of the precursor shock with the right wall).

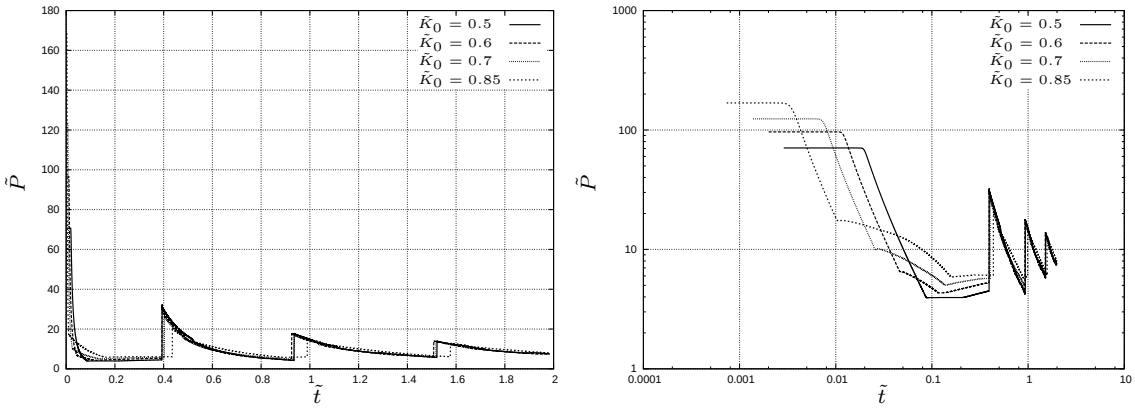

Figure 9: Detonation initiation due to the shock reflection. $\tilde{P}$ versus $\tilde{t}$ on the right wall in different cases. Here we take as $t = 0$ the instant in which there is the impact of the precursor shock with the right wall. (Non-dimensional values).

As one can see (and as already mentioned before), the larger the value of $\tilde{K}_0$, the larger the maximum overpressure, the lower the duration of the action of this overpressure on the right wall. Indeed, the maximum value corresponds to the burnt state behind the detonation wave generated by the precursor shock reflection. The value of $\tilde{\Delta t}$ decreases as the flame speed increases while the value of the pressure in the burnt region of the detonation increases as the flame speed increases. Once the left travelling detonation wave interacts with the right travelling flame, we expect the generation of a left travelling shock and a right travelling deflagration wave, which is responsible of the pressure decreasing on the wall. As one can see in Figure 8, the distance that the right travelling rarefaction wave has to last decreases with $\tilde{K}_0$ while its speed, the sound speed behind the detonation wave, increases with $\tilde{K}_0$. This explains why the larger the value of $\tilde{K}_0$, the lower the duration of the action of this overpressure on the right wall.

3.4 Comparison of the different combustion regimes (with the same fundamental flame speed)

It is also interesting to compare the different combustion regimes with the same value of the fundamental flame speed. For the sake of brevity, we restrict our attention to the case

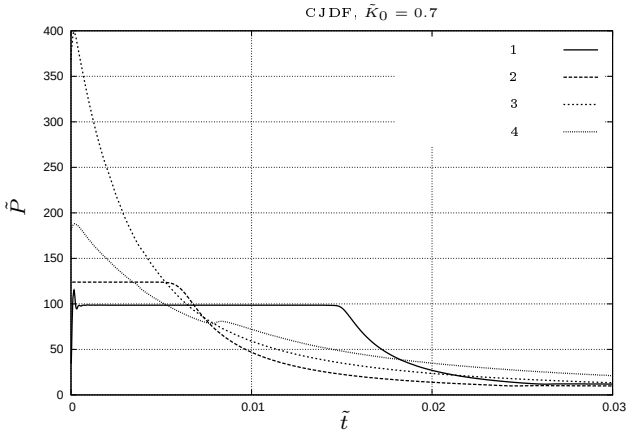

Figure 10: 1D DDT. $\tilde{K}_0 = 0.7$. Comparison of the different cases. 1 = deflagration, 2 = detonation initiation at the wall, 3 = deflagration-to-detonation transition at the flame with $\tilde{L}_d = \tilde{L}_{d,\mathrm{foc}}$, 4 = deflagration-to-detonation transition at the flame with $\tilde{L}_d = 0.9\tilde{L}_{d,\mathrm{foc}}$. Pressure at the right extremity as function of time. (Non-dimensional values).

$\tilde{K_0} = 0.7$ and $\tilde{t} < 0.03$. In Figure 10 we represent, for this case, the pressure $\tilde{P}$ as function of the time $\tilde{t}$ at the right extremity ($\tilde{t} = 0$ corresponds to the case in which the "first" shock interacts with the right extremity). As one can see, the case of DDT at the flame with simultaneous reflection of the precursor shock and the detonation at the right wall (i.e. $\tilde{L_d} = \tilde{L}_{d,\text{foc}}$) presents both the maximum overpressure and the maximum positive impulse. From a qualitative point of view, this case seems to be the most dangerous from a mechanical point of view. Nevertheless, the best way to compare all this cases is to analyze their action over the mechanical structure we have to deal with.

4 Fluid-structure interaction

4.1 Infinite cylinder investigation

If we consider the infinite cylinder in elastic regime, the first frequency is

$$f = \frac{1}{2\pi R}\sqrt{\frac{E}{\rho(1-\nu^2)}} \approx 2613 \text{ Hz}$$

i.e. the first period is 0.383 ms. The time we use to non-dimensionalize the results of Section 3 (i.e. the unit time in the figures of Section 3) is $L/\sqrt{R_u T_0}$, i.e. 24.2 ms; then the first period is 0.015 times $L/\sqrt{R_u T_0}$. It follows that the characteristic time for the structure has the same order of magnitude of the characteristic times of the loads acting on the right extremity, which are represented in Figure 10. This implies that, from a mechanical point of view, we have to perform a dynamic analysis of the device. Then, as mention in Section 2.3, point 2, we apply the loads obtained in the right extremity of the tube to the infinite cylinder. In the case of reflection of a constant speed deflagration wave, the maximum deformation (strain ϵ) is 1.3% (plastic region of Figure 1) and occurs for $\tilde{K_0} = 0.7$. In the case of "slow deflagration"-to-detonation transition at the flame, the maximum deformation is 0.5% and occurs as the detonation transition occurs at $\tilde{L_d} = 0.85$. In the case of "fast deflagration"-to-detonation transition at the flame, the maximum deformation is 3.7% and corresponds to the case $\tilde{K_0} = 0.5$ and $\tilde{L_d} = 0.9\tilde{L}_{d,\text{foc}}$ (the detonation transition occurs such that the precursor shock of the flame and the detonation wave reach the right wall at the same time). Finally, in case of detonation initiation due to the shock reflection at the right wall, we obtain a maximum deformation of 1.2 % corresponding to $\tilde{K_0} = 0.7$.

4.2 Mechanical device investigation

According to these results, using Europlexus, in the mechanical device we compute a DDT, namely a detonation in which the initial condition corresponds to a deflagration wave with $\tilde{K_0} = 0.5$, such that the precursor shock of the deflagration and the detonation wave arrives at the right wall at the same time. In this case we obtained almost everywhere a plastic deformation lower than 3.7% except in the the junction between the the ellipse and the cylinder. Here the plastic deformation becomes about 19%.

5 Conclusion

According the hypotheses here performed, we have evaluated the stress and strain in a mechanical device subjected to different combustion regimes, in particular to a deflagration-to-detonation transition in which the precursor shock of the deflagration and the detonation are simultaneously reflected by the wall opposite to the region in which the deflagration is initiated.

In order to provide accurate results, several hypotheses have been performed, which always maximize the pressure load acting on the mechanical device. For instance, we have supposed that the left extremity of the device is closed, while in the reality it is open. This increases the effects of the pressure load on the mechanical device.
We emphasize that this combustion regime is quite theoretical (flame speed of the deflagration high, simultaneous reflection of the detonation and the deflagration precursor shock). We could provide more realistic loads, if we knew some physical quantities, like the flame speed and the so-called run-up distance; nevertheless the only way of having these quantities is to perform (physical) experiments on the considered geometry.

Acknowledgment

This work has been partially supported by the Institut Laue-Langevin, or ILL (Grenoble, France). The authors are grateful to Jean Paul Bidet for the fruitful discussions.

References

[1] Ciccarelli G. and Dorofeev S. Flame acceleration and transition to detonation in ducts. *Progress in Energy and Combustion Science* 2008; **34**: 499-550.

[2] RCC-MX code. Règles de Conception et de Construction des Matériels Mécaniques des Réacteurs Expérimentaux, de leurs auxiliaires et des dispositifs d'irradiation. CEA Edition, 2008.

[3] Beccantini A. and Studer E. The reactive Riemann problem for thermally perfect gases at all combustion regimes. *International Journal for Numerical Methods in Fluids.* 2009.

[4] Chaumeix N. and Paillard C.E. Évaluation des risques pour le transport d'hydrogène énergie pur ou en mélange avec le gas naturel. Technical report ANR-06-PANH-001-02. 2008

[5] Li J., Zhao Z., Kazakov A., Dryer F.L. An Updated Comprehensive Kinetic Model of Hydrogen Combustion. International Journal of Chemical Kinetics. Vol. 36, p. 566-575. 2004

[6] Meister A. Asymptotic single and multiple scale expansions in the low Mach number limit. *SIAM J. Appl. Math.*, **60**: 256-271. 2000

[7] Le Métayer O., Massoni J., Saurel R. Modelling evaporation fronts with reactive Riemann solvers. *Journal of Computational Physics* 2005; **205**: 567-610.

[8] Abgrall R., Saurel R. Discrete equations for physical and numerical compressible multiphase mixtures. *Journal of Computational Physics* 2003; **186**: 361-396.

[9] Europlexus. A Computer Program for the Numerical Simulation of Fluid-Structure Systems under Transient Dynamic Loading.
http://europlexus.jrc.ec.europa.eu

[10] Kuhl A.L., Kamel M.M., Oppenheim A.K. Pressure Waves Generated by Steady Flames. *Proceedings of the Combustion Institute* 1973; **14**: 1201-1215.

[11] Chan CK, WA Dewitt WA. Deflagration-to-detonation transition in end gases. Symposium (International) on Combustion, Volume 26, Issue 2, Pages 2679-2684. 1996